

# Synthesis, Characterization, Crystal Structures and Antimicrobial Activity of Oxidovanadium(V) Complexes with Mixed Ligands

X. Q. Luo<sup>a</sup>, Y. J. Han<sup>a</sup>, and L. W. Xue<sup>a,\*</sup>

<sup>a</sup>College of Chemistry and Chemical Engineering, Pingdingshan University, Pingdingshan Henan, 467000 P.R. China

\*e-mail: pdsuchemistry@163.com

Received November 25, 2018; revised August 22, 2019; accepted August 26, 2019

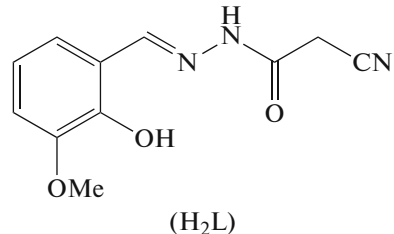
**Abstract**—Two new oxidovanadium(V) complexes,  $[\text{VOLL}^1]$  (**I**) and  $[\text{VOLL}^2]$  (**II**), where L is the dianionic form of the hydrazone ligand 2-cyano-*N*-(2-hydroxy-3-methoxybenzylidene)acetohydrazide ( $\text{H}_2\text{L}$ ),  $\text{L}^1$  and  $\text{L}^2$  are the deprotonated form of 2-hydroxybenzohydroxamate ( $\text{HL}^1$ ) and 3-hydroxy-2-methyl-4*H*-pyran-4-one ( $\text{HL}^2$ ), respectively, have been prepared and characterized by elemental analyses, IR, UV-Vis, <sup>1</sup>H NMR and single crystal X-ray crystallographic determination (CIF files CCDC nos. 1880992 (**I**) and 1880993 (**II**)). The V atoms in the complexes are in octahedral coordination with the hydrazone ligand coordinates to the metal atoms through the phenolate O, imino N and enolate O atoms, and with 2-hydroxybenzohydroxamate and 3-hydroxy-2-methyl-4*H*-pyran-4-one through the carbonyl and hydroxyl O atoms. The effect of the compounds on the antimicrobial activity against *Staphylococcus aureus*, *Escherichia coli*, and *Candida albicans* was studied.

**Keywords:** hydrazone, vanadium complex, mixed ligands, crystal structure, antimicrobial activity

**DOI:** 10.1134/S1070328420010054

## INTRODUCTION

Schiff bases with typical azomethine groups, C=N, are interesting ligands in coordination chemistry [1–3]. In recent years, metal complexes of Schiff bases have attracted remarkable attention due to their versatile biological activity, such as antifungal, antibacterial and antitumor [4–6]. Schiff base complexes derived from salicylaldehyde and its derivatives with primary amines, bearing the  $\text{N}_2\text{O}$ ,  $\text{N}_2\text{S}$ ,  $\text{NO}_2$  or  $\text{NSO}$  donor sets, have particular biological activities [7–9]. Hydroxamic acids and Pyrone compounds are bidentate ligands in various metal complexes [10–12]. Most complexes with such ligands have interesting biological properties [13–15]. Hydrazone compounds belong to Schiff base family, which are of particular interest in biological chemistry [16, 17]. In the present work, two new oxidovanadium(V) complexes,  $[\text{VOLL}^1]$  (**I**) and  $[\text{VOLL}^2]$  (**II**), where L is the dianionic form of the hydrazone ligand 2-cyano-*N*-(2-hydroxy-3-methoxybenzylidene)acetohydrazide ( $\text{H}_2\text{L}$ ),  $\text{L}^1$  and  $\text{L}^2$  are the deprotonated form of 2-hydroxybenzohydroxamate ( $\text{HL}^1$ ) and 3-hydroxy-2-methyl-4*H*-pyran-4-one ( $\text{HL}^2$ ), respectively, are reported.



## EXPERIMENTAL

**Material and methods.** 3-Methoxysalicylaldehyde, cyanoacetohydrazide,  $\text{HL}^1$ , and  $\text{HL}^2$  were purchased from Fluka. Other reagents and solvents were analytical grade and used without further purification. Elemental (C, H, and N) analyses were made on a Perkin-Elmer Model 240B automatic analyser. Infrared (IR) spectra were recorded on an IR-408 Shimadzu 568 spectrophotometer. UV-Vis spectra were recorded on a Lambda 35 spectrometer. <sup>1</sup>H NMR spectra were recorded on a Bruker 300 MHz instrument. X-ray diffraction was carried out on a Bruker SMART 1000 CCD area diffractometer.

**Synthesis of  $\text{H}_2\text{L}$ .** 3-Methoxysalicylaldehyde (0.152 g, 1.0 mmol) was dissolved in methanol (20 mL), to which was added dropwise a methanol solution (20 mL) containing cyanoacetohydrazide (0.099 g, 1.0 mmol). The mixture was stirred at ambi-

ent temperature for 1 h. Then the methanol was evaporated by distillation, yielding yellow solid product of  $H_2L$ . The product was recrystallized from methanol to give pure product of  $H_2L$ .

For  $C_{11}H_{11}N_3O_3$

Anal. calcd., %	C, 56.6	H, 4.8	N, 18.0
Found, %	C, 56.8	H, 4.7	N, 18.2

IR data (KBr;  $\nu$ ,  $\text{cm}^{-1}$ ): 3445 (OH), 3257 (NH), 2260 (C≡N), 1681 (C=O), 1612 (C=N). UV-Vis data in methanol ( $\lambda_{\text{max}}$ , nm ( $\epsilon$ ,  $\text{L mol}^{-1} \text{cm}^{-1}$ )): 225, 15878; 287, 15510; 325, 5430.  $^1\text{H}$  NMR (300 MHz;  $d^6$ -DMSO;  $\delta$ , ppm): 9.16 (d., 1H, ArH), 8.48 (s., 1H, CH=N), 7.38 (t., 1H, ArH), 7.27 (d., 1H, ArH), 7.03 (d., 1H, ArH), 6.33 (d., 1H, ArH), 3.81 (s., 3H,  $CH_3$ ), 3.17 (s., 2H,  $CH_2$ ), 2.24 (s., 1H,  $CH_3$ ).

**Synthesis of complex I.** The hydrazone  $H_2L$  (23.3 mg, 0.1 mmol) and  $HL^1$  (15.3 mg, 0.1 mmol) were dissolved by methanol (10 mL), to which was added with stirring a methanol solution (10 mL) of  $VO(\text{Acac})_2$  (26.5 mg, 0.1 mmol). The mixture was stirred for 1 h at ambient temperature to give a deep brown solution. Brown block-shaped single crystals suitable for X-ray diffraction were formed by slow evaporation of the solution in air for several days. The yield was 45% (based on V).

For  $C_{18}H_{15}N_4O_7V$

Anal. calcd., %	C, 48.0	H, 3.4	N, 12.4
Found, %	C, 47.8	H, 3.3	N, 12.6

IR data (KBr;  $\nu$ ,  $\text{cm}^{-1}$ ): 3351 (OH), 3195 (NH), 2261 (C≡N), 1610 (C=N), 973 (V=O). UV-Vis data in methanol ( $\lambda_{\text{max}}$ , nm ( $\epsilon$ ,  $\text{L mol}^{-1} \text{cm}^{-1}$ )): 235, 16110; 266, 13235; 346, 4450; 470, 5022.  $^1\text{H}$  NMR (300 MHz;  $d^6$ -DMSO;  $\delta$ , ppm): 9.06 (s., 1H, NH), 8.45 (s., 1H, CH=N), 7.55 (d., 1H, ArH), 7.43 (t., 1H, ArH), 7.33 (d., 1H, ArH), 7.20 (t., 1H, ArH), 7.01–6.85 (m., 3H, ArH), 3.82 (s., 3H,  $CH_3$ ), 3.17 (s., 2H,  $CH_2$ ).

**Synthesis of compound II.** The hydrazone  $H_2L$  (23.3 mg, 0.1 mmol) and  $HL^2$  (12.6 mg, 0.1 mmol) were dissolved by methanol (10 mL), to which was added with stirring a methanol solution (10 mL) of  $VO(\text{Acac})_2$  (26.5 mg, 0.1 mmol). The mixture was stirred for 1 h at ambient temperature to give a deep brown solution. Brown block-shaped single crystals suitable for X-ray diffraction were formed by slow evaporation of the solution in air for several days. The yield was 32% (based on V).

For  $C_{17}H_{14}N_3O_7V$

Anal. calcd., %	C, 48.2	H, 3.3	N, 9.9
Found, %	C, 48.3	H, 3.4	N, 10.0

IR data (KBr;  $\nu$ ,  $\text{cm}^{-1}$ ): 2261 (C≡N), 1610 (C=N), 972 (V=O). UV-Vis data in methanol ( $\lambda_{\text{max}}$ , nm ( $\epsilon$ ,  $\text{L mol}^{-1} \text{cm}^{-1}$ )): 215, 17230; 273, 14115; 350, 4150; 476, 3832.  $^1\text{H}$  NMR (300 MHz;  $d^6$ -DMSO;  $\delta$ , ppm): 9.16 (d., 1H, ArH), 8.48 (s., 1H, CH=N), 7.38 (t., 1H, ArH), 7.27 (d., 1H, ArH), 7.03 (d., 1H, ArH), 6.33 (d., 1H, ArH), 3.81 (s., 3H,  $CH_3$ ), 3.17 (s., 2H,  $CH_2$ ), 2.24 (s., 1H,  $CH_3$ ).

**X-ray structure determination.** Data were collected from selected crystals mounted on glass fibres. The data for the two complexes were processed with SAINT [18] and corrected for absorption using SADABS [19]. Multi-scan absorption corrections were applied with  $\psi$ -scans [20]. The structures were solved by direct methods using the program SHELXS-97 and were refined by full-matrix least-squares techniques on  $F^2$  using anisotropic displacement parameters [21]. The amino H atom in complex I was located from an electronic map and refined with N–H distance of 0.90(1) Å. The remaining hydrogen atoms were placed at the calculated positions. Idealized H atoms were refined with isotropic displacement parameters set to 1.2 (1.5 for methyl groups) times the equivalent isotropic  $U$  values of the parent atoms. The crystallographic data for the complexes are listed in Table 1, selected bond lengths and bond angles for compounds I and II are given in Table 2.

Supplementary material for structures has been deposited with the Cambridge Crystallographic Data Centre (CCDC 1880992 (I) and 1880993 (II); deposit@ccdc.cam.ac.uk or <http://www.ccdc.cam.ac.uk>).

## RESULTS AND DISCUSSION

The hydrazone compound  $H_2L$  was prepared by the condensation of equimolar quantities of 3-methoxysalicylaldehyde with cyanoacetohydrazide in methanol. The hydrazone compound prepared in this way was formed in nearly quantitative yield and is of high purity. Complexes I and II were readily synthesized by reaction of the hydrazone compound  $H_2L$  with  $VO(\text{Acac})_2$  in methanol in the presence of  $HL^1$  and  $HL^2$ , respectively. All the compounds are very stable at room temperature in the solid state, and soluble in common organic solvents, such as methanol, ethanol, and acetonitrile. The results of the elemental analyses are in accord with the composition suggested for the hydrazone and the complexes.

For the IR spectrum of  $H_2L$ , the typical band indicative of the azomethine group was observed at 1612  $\text{cm}^{-1}$ , while in the complexes, it was observed at 1610  $\text{cm}^{-1}$  for I and 1596  $\text{cm}^{-1}$  for II [22]. The strong absorption at 1681  $\text{cm}^{-1}$  in the spectrum of  $H_2L$  is assigned to the stretching vibration of the C=O bond. The weak absorptions at 3445  $\text{cm}^{-1}$  for  $H_2L$  and 3351  $\text{cm}^{-1}$  for I can be attributed to the vibration of O–

**Table 1.** Crystallographic data and refinement parameters for complexes **I** and **II**

Parameters	Value	
	<b>I</b>	<b>II</b>
Habit, color	Block, brown	Block, brown
Formula weight	450.28	423.25
Temperature, K	298(2)	298(2)
Crystal size, mm	0.17 × 0.15 × 0.15	0.15 × 0.13 × 0.12
Radiation ( $\lambda$ , Å)	MoK $\alpha$ (0.71073)	MoK $\alpha$ (0.71073)
Crystal system	Monoclinic	Triclinic
Space group	$P2_1/c$	$P\bar{1}$
Unit cell dimensions:		
$a$ , Å	13.568(2)	8.3872(8)
$b$ , Å	18.616(4)	8.9453(9)
$c$ , Å	7.797(1)	12.3034(11)
$\alpha$ , deg	90	93.071(1)
$\beta$ , deg	105.696(3)	102.172(1)
$\gamma$ , deg	90	103.545(2)
$V$ , Å <sup>3</sup>	1895.8(6)	872.06(14)
$Z$	4	2
$\rho_{\text{calcd}}$ , g cm <sup>-3</sup>	1.578	1.612
$F(000)$	920	432
Absorption coefficient, mm <sup>-1</sup>	0.574	0.617
$\theta$ Range for data collection, deg	1.90–24.70	1.70–25.50
Index ranges, $h, k, l$	$-15 \leq h \leq 10$ , $-21 \leq k \leq 19$ , $-9 \leq l \leq 9$	$-10 \leq h \leq 10$ , $-7 \leq k \leq 10$ , $-14 \leq l \leq 14$
Reflections collected	9173	4613
Independent reflections	3210	3209
Data ( $I > 2\sigma(I)$ ), parameters	2401, 276	2804, 254
Restraints	1	0
Final $R$ indices ( $I > 2\sigma(I)$ )	$R_1 = 0.0397$ , $wR_2 = 0.1016$	$R_1 = 0.0336$ , $wR_2 = 0.0871$
$R$ indices (all data)	$R_1 = 0.0603$ , $wR_2 = 0.1129$	$R_1 = 0.0405$ , $wR_2 = 0.0917$
Goodness-of-fit on $F^2$	1.015	1.056

H groups, and those at 3257 cm<sup>-1</sup> for H<sub>2</sub>L and 3195 cm<sup>-1</sup> for **I** can be attributed to the vibration of N–H groups. The bands at 2260 cm<sup>-1</sup> for H<sub>2</sub>L and the complexes are due to the vibration of the C≡N groups. The bands indicative of the V=O groups of the complexes are observed at about 973 cm<sup>-1</sup> [23].

UV-Vis spectra of H<sub>2</sub>L and the complexes were carried out in methanol. In the spectrum of the hydrazone, the band centered at 325 nm is attributed to the azomethine chromophore  $\pi$ – $\pi^*$ -transition. The band at higher energy (287 nm) is associated with the benzene  $\pi$ – $\pi^*$ -transition. In the spectra of the complexes, the bands at 470–476 nm are attributed to the intra-

molecular charge transfer transitions from the  $p_{\pi}$  orbital on the phenolate O to the empty  $d$  orbitals of the V atoms [24].

The molecular structures of complexes **I** and **II** are shown in Fig. 1. The V atoms are coordinated by one hydrazone ligand, one oxo O group, and one secondary ligand, viz. HL<sup>1</sup> for **I** and HL<sup>2</sup> for **II**. The hydrazone ligand coordinated to the V atom through the phenolate O, imino N, and enolate O atoms. The secondary ligands coordinated to the V atoms through the deprotonated hydroxyl O and carbonyl O atoms. The V atoms are in octahedral coordination with the three donor atoms of the hydrazone ligand and the hydroxyl O atom of the secondary ligand defining the equatorial

**Table 2.** Selected bond lengths (Å) and bond angles (deg) for complexes **I** and **II**

Bond	<i>d</i> , Å	Bond	<i>d</i> , Å		
<b>I</b>					
V(1)–O(7)	1.580(2)	V(1)–O(5)	1.8584(18)		
V(1)–O(1)	1.8711(19)	V(1)–O(2)	1.9786(19)		
V(1)–N(1)	2.075(2)	V(1)–O(4)	2.1822(18)		
<b>II</b>					
V(1)–O(7)	1.5880(17)	V(1)–O(1)	1.8415(15)		
V(1)–O(5)	1.8722(14)	V(1)–O(2)	1.9584(15)		
V(1)–N(1)	2.0931(18)	V(1)–O(4)	2.2595(16)		
Angle	$\omega$ , deg	Angle	$\omega$ , deg		
<b>I</b>					
O(7)V(1)O(5)	94.26(9)	O(7)V(1)O(1)	99.23(11)		
O(5)V(1)O(1)	109.06(8)	O(7)V(1)O(2)	101.22(11)		
O(5)V(1)O(2)	87.79(8)	O(1)V(1)O(2)	152.37(9)		
O(7)V(1)N(1)	97.22(10)	O(5)V(1)N(1)	160.45(9)		
O(1)V(1)N(1)	84.68(9)	O(2)V(1)N(1)	74.51(8)		
O(7)V(1)O(4)	169.60(9)	O(5)V(1)O(4)	75.97(7)		
O(1)V(1)O(4)	80.97(8)	O(2)V(1)O(4)	82.22(8)		
N(1)V(1)O(4)	93.16(8)	<b>II</b>			
O(7)V(1)O(1)	99.23(9)	O(7)V(1)O(5)	98.23(8)		
O(1)V(1)O(5)	103.19(7)	O(7)V(1)O(2)	100.45(8)		
O(1)V(1)O(2)	152.18(8)	O(5)V(1)O(2)	93.24(6)		
O(7)V(1)N(1)	97.13(8)	O(1)V(1)N(1)	83.73(7)		
O(5)V(1)N(1)	161.88(7)	O(2)V(1)N(1)	74.50(7)		
O(7)V(1)O(4)	175.36(7)	O(1)V(1)O(4)	80.53(7)		
O(5)V(1)O(4)	77.37(6)	O(2)V(1)O(4)	81.40(7)		
N(1)V(1)O(4)	87.46(6)				

plane, and with the carbonyl O atom of the secondary ligand, and the oxo O group occupying the axial positions. The bond distances subtended at the V atoms are comparable to each other, and also similar to those observed in the similar vanadium complexes with hydrazones [25, 26]. The *cis* and *trans* coordinate bond angles are range from 74.51(8) $^{\circ}$  to 109.06(8) $^{\circ}$  and from 152.37(9) $^{\circ}$  to 169.60(9) $^{\circ}$  for **I**, and from 74.50(7) $^{\circ}$  to 103.19(7) $^{\circ}$  and from 152.18(8) $^{\circ}$  to 175.36(7) $^{\circ}$  for **II**, respectively, indicating the distortion of the octahedral coordination from ideal geometry. Molecular packing structure of complexes **I** and **II** are shown in Fig. 2. The molecules in complex **I** are linked through N–H $\cdots$ O, O–H $\cdots$ O, and C–H $\cdots$ O hydrogen bonds (Table 3) to form a three-dimensional network.

The molecules in complex **II** are stack along the *x*-axis direction.

Qualitative determination of antimicrobial activity was done using the disk diffusion method [27]. The results are summarized in Table 4. A comparative study of minimum inhibitory concentration (MIC) values of the hydrazone and the complexes indicates that the complexes have better activity than the free hydrazone. Generally, this is caused by the greater lipophilic nature of the complexes than the ligand. Such increased activity of the metal chelates can be explained on the basis of chelating theory [28]. On chelating, the polarity of the metal atoms will be reduced to a greater extent due to the overlap of the ligand orbital and partial sharing of positive charge of the metal atoms with donor atoms. Further, it

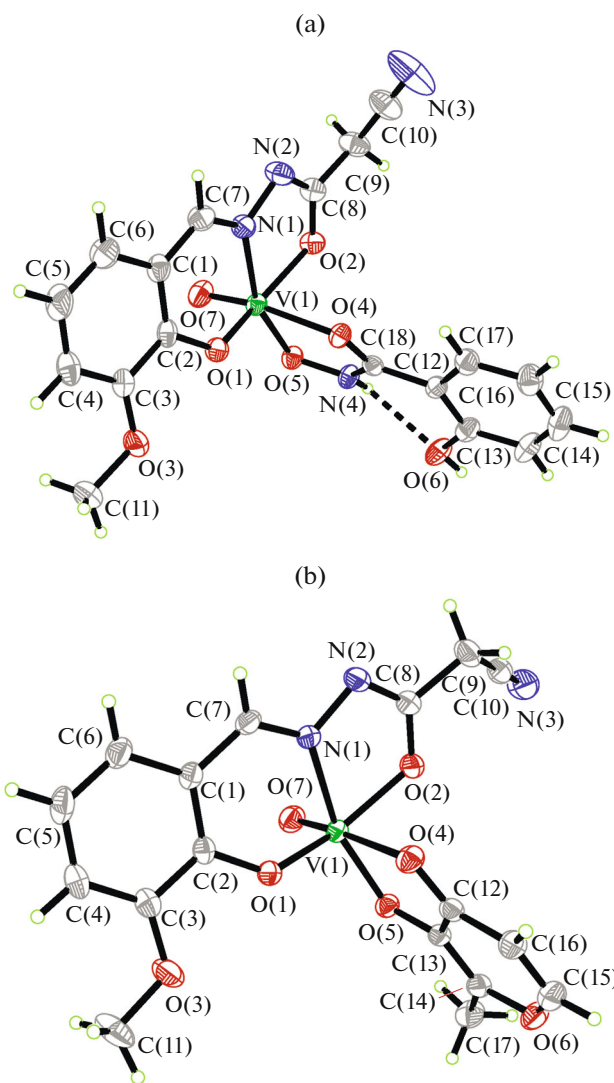


**Fig. 1.** Perspective view of complexes **I** (a) and **II** (b) with 30% probability thermal ellipsoids.

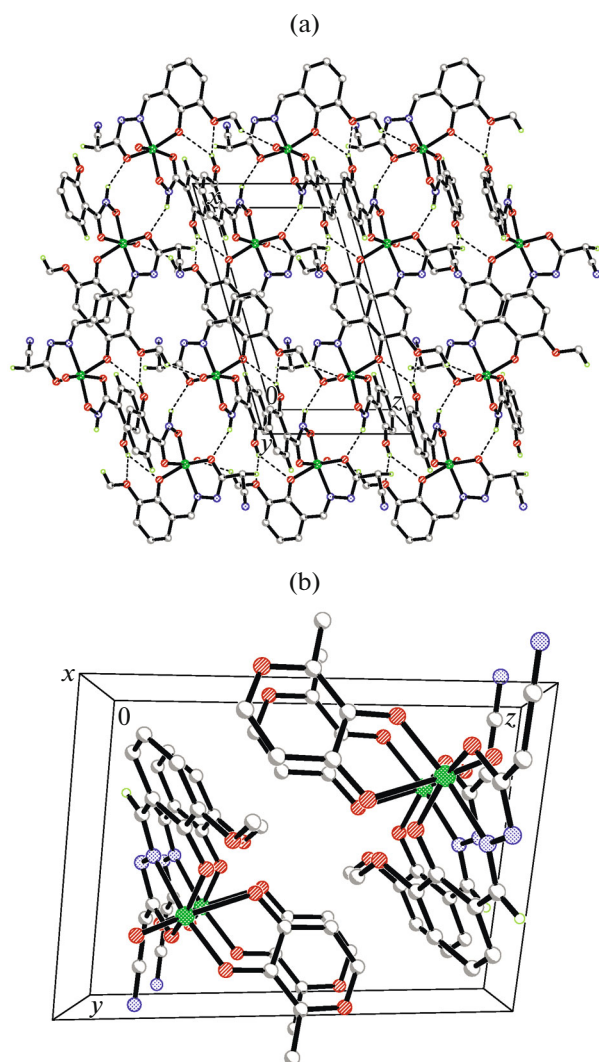


**Fig. 2.** Molecular packing structure of complexes **I** (a) and **II** (b) with hydrogen bonds drawn as dashed lines.

**Table 3.** Distances (Å) and angles (deg) involving hydrogen bonding of complexes **I** and **II**\*

D–H···A	Distance, Å			Angle $D$ –H··· $A$ , deg
	$D$ –H	H··· $A$	$D$ ··· $A$	
<b>I</b>				
N(4)–H(4)···O(6)	0.90(1)	2.18(3)	2.668(3)	113
N(4)–H(4)···O(2) <sup>#1</sup>	0.90(1)	2.05(2)	2.873(3)	152
O(6)–H(6)···O(1) <sup>#2</sup>	0.82	2.44	3.049(3)	132
O(6)–H(6)···O(3) <sup>#3</sup>	0.82	2.11	2.883(3)	157
C(9)–H(9B)···O(4) <sup>#3</sup>	0.97	2.58	3.378(3)	139
C(11)–H(11B)···O(7) <sup>#4</sup>	0.96	2.55	3.185(3)	124
<b>II</b>				
C(7)–H(7)···O(7) <sup>#5</sup>	0.93	2.60	3.198(3)	123

\* Symmetry codes: <sup>#1</sup>  $-x, -y, -z$ ; <sup>#2</sup>  $-x, -y, 1-z$ ; <sup>#3</sup>  $x, y, -1+z$ ; <sup>#4</sup>  $x, y, 1+z$ ; <sup>#5</sup>  $1-x, 1-y, -z$ .

**Table 4.** MIC values ( $\mu\text{g/mL}$ ) for the antimicrobial activities of the tested compounds

Compounds	<i>Staphylococcus aureus</i>	<i>Escherichia coli</i>	<i>Candida albicans</i>
H <sub>2</sub> L	64	16	>512
<b>I</b>	2.0	1.0	64
<b>II</b>	8.0	2.0	64
Tetracycline	0.32	2.12	>1024

increases the delocalization of *p*-electrons over the whole chelate ring and enhances the lipophilicity of the complexes. This increased lipophilicity enhances the penetration of the complexes into lipid membrane and blocks the metal binding sites on enzymes of micro-organisms.

From the results, it is obvious that the two complexes have higher antibacterial and antifungi activities against *Staphylococcus aureus*, *Escherichia coli*, and *Candida albicans* when compared to the free hydrazone. Complex **II** has stronger activity against *Staphylococcus aureus* and *Escherichia coli* than complex **I**. The complexes have strong activity against *Escherichia coli*, with MIC value of 1.0–2.0  $\mu\text{g/mL}$ , which is superior to Tetracycline. It is interesting that both complexes have medium activity against *Candida albicans*, which is rarely seen in metal complexes.

#### FUNDING

This research was supported by the Top-class foundation of Pingdingshan University (nos. PXY-BSQD-2018006 and PXY-PYJJ-2018002).

#### REFERENCES

- Burlov, A.S., Vlasenko, V.G., Koshchienko, Y.V., et al., *Polyhedron*, 2018, vol. 154, p. 65.
- Salman, Y., Barlas, F.B., Yavuz, M., et al., *Inorg. Chim. Acta*, 2018, vol. 483, p. 98.
- Muche, S., Harms, K., Biernasiuk, A., et al., *Polyhedron*, 2018, vol. 151, p. 465.
- Valentova, J., Varenyi, S., Herich, P., et al., *Inorg. Chim. Acta*, 2018, vol. 480, p. 16.
- Soliman, S.M., El-Faham, A., Elsilk, S.E., et al., *Inorg. Chim. Acta*, 2018, vol. 479, p. 275.
- Nithya, P., Rajamanikandan, R., Simpson, J., et al., *Polyhedron*, 2018, vol. 145, p. 200.
- Jana, K., Das, S., Maity, T., et al., *J. Coord. Chem.*, 2018, vol. 71, no. 10, p. 1497.
- Qian, H.Y., *Russ. J. Coord. Chem.*, 2018, vol. 44, no. 1, p. 32.
- Ribeiro, N., Roy, S., Butenko, N., et al., *J. Inorg. Biochem.*, 2017, vol. 174, p. 63.
- Silver, M.A., Cary, S.K., Stritzinger, J.T., et al., *Inorg. Chem.*, 2016, vol. 55, no. 11, p. 5092.
- Orlowska, E., Roller, A., Wiesinger, H., et al., *RSC Adv.*, 2016, vol. 6, no. 46, p. 40238.
- Vishwakarma, P.K., Mir, J.M., and Maurya, R.C., *J. Chem. Sci.*, 2016, vol. 128, no. 4, p. 511.
- Failes, T.W., Hall, M.D., and Hambley, T.W., *Dalton Trans.*, 2003, no. 8, p. 1596.
- Sheng, G.H., Huo, Y., Ye, Y.T., et al., *Russ. J. Coord. Chem.*, 2014, vol. 40, no. 9, p. 664. <https://doi.org/10.1134/S1070328414090085>
- Sharma, N., Kumari, M., Kumar, V., et al., *J. Coord. Chem.*, 2010, vol. 63, no. 11, p. 1940.
- Soujanya, M., Rajitha, G., Umamaheswari, A., et al., *Lett. Drug Des. Discov.*, 2018, vol. 15, no. 8, p. 875.
- Kumar, S.S., Biju, S., and Sadasivan, V., *J. Mol. Struct.*, 2018, vol. 1156, p. 201.
- SMART and SAINT. Area Detector Control and Integration Software*, Madison: Bruker Analytical X-ray Instruments Inc., 1997.
- Sheldrick, G.M., *SADABS. Program for Empirical Absorption Correction of Area Detector Data*, Göttingen: Univ. of Göttingen, 1997.
- North, A.C.T., Phillips, D.C., and Mathews, F.S., *Acta Crystallogr., Sect. A*, 1968, vol. 24, no. 3, p. 351.
- Sheldrick, G.M., *SHELXL-97. Program for the Refinement of Crystal Structures*, Göttingen: Univ. of Göttingen, 1997.
- Sarkar, A. and Pal, S., *Polyhedron*, 2006, vol. 25, no. 7, p. 1689.
- Sarkar, A. and Pal, S., *Inorg. Chim. Acta*, 2008, vol. 361, no. 8, p. 2296.
- Asgedom, G., Sreedhara, A., Kivikoski, J., et al., *Dalton Trans.*, 1996, no. 1, p. 93.
- Guo, S.H., Sun, N., Ding, Y.W., et al., *Z. Anorg. Allg. Chem.*, 2018, vol. 644, no. 19, p. 1172.
- Li, L., Lv, K.-W., Li, Y.-T., et al., *Chin. J. Inorg. Chem.*, 2017, vol. 33, no. 5, p. 905.
- Rosu, T., Negoiu, M., and Pasculescu, S., *Eur. J. Med. Chem.*, 2010, vol. 45, no. 2, p. 774.
- Searl, J.W., Smith, R.C., and Wyard, S.J., *Proc. Phys. Soc. London*, 1961, vol. 78, no. 505, p. 1174.